Chemistry & Biology, Vol. 9, 881–889, August, 2002, ©2002 Elsevier Science Ltd. All rights reserved. PII S1074-5521(02)00183-7

Interference with Heme Binding to Histidine-Rich Protein-2 as an Antimalarial Strategy

Clara Y.H. Choi,[1] Eric L. Schneider,[4] Jin M. Kim,[4] Ilya Y. Gluzman,[3] Daniel E. Goldberg,[3] Jonathan A. Ellman,[4] and Michael A. Marletta[1,2,4,5]
[1]Department of Biological Chemistry
Howard Hughes Medical Institute and
[2]Department of Medicinal Chemistry
University of Michigan
Ann Arbor, Michigan 48109
[3]Department of Molecular Microbiology and
Howard Hughes Medical Institute
Washington University School of Medicine
St. Louis, Missouri 63110
[4]Department of Chemistry
University of California, Berkeley
Berkeley, California 94720

Summary

The erythrocytic growth stage of *Plasmodium falciparum* involves hemoglobin proteolysis as the primary nutrient source with the concomitant release of free heme. The liberated heme is processed by the parasite into hemozoin, a polymeric porphyrin dimer. Histidine-rich protein binds heme and mediates the formation of hemozoin, which is inhibited by the antimalarial drug chloroquine. Interference with heme binding was determined using a microtiterplate assay. Combinatorial libraries were screened and tested against parasite growth, revealing a good correlation between heme binding interference and the inhibition of parasite growth. Several of these compounds retain their potency against a chloroquine-resistant strain of *Plasmodium falciparum*. The most potent compounds have IC_{50} values less than or equal to 50 nM against chloroquine-resistant and chloroquine-sensitive parasites.

Introduction

Malaria is one of the most deadly infectious diseases in the world, responsible for close to two million deaths per year. Aminoquinoline-based compounds have been effective in the treatment of the disease; however, drug-resistant parasites have emerged to the most commonly used aminoquinoline, chloroquine. More ominous is the appearance of multidrug-resistant organisms, making development of novel antimalarial drugs imperative [1].

The life cycle of the malaria parasite is complex and includes both an *Anopheles* mosquito and a human host. For a portion of the life cycle, the malaria parasite develops within human red blood cells, and it is during this intraerythrocytic stage that many of the clinical symptoms associated with malaria, including recurring fever, chills, and anemia are observed. The most deadly of all malaria parasites is *Plasmodium falciparum*. Adherence of infected erythrocytes to the vascular endothelium of postcapillary venules, especially in the brain, can lead to severe clinical complications [2].

During the intraerythrocytic stage, the host hemoglobin is a primary food source of the parasite. Hemoglobin degradation takes place inside the parasite's food vacuole. Upon hemoglobin proteolysis, toxic free heme is released. Heme is ultimately sequestered by formation of hemozoin, originally described as a polymer of heme (malaria pigment) and recently characterized as an insoluble dimer linked via iron-carboxylate coordination bonds and further complexed by hydrogen bonds to another dimer [3]. This highly unusual method of heme detoxification allows the parasite to deal with high concentrations of cytotoxic free heme that is generated inside the food vacuole [4].

Many of the antimalarial drugs act exclusively on the blood stage of the infection. Quinacrine [6-chloro-9-(4-diethylamino-1-methylbutylamino)-2-methoxyacridine] and quinoline-containing drugs, such as chloroquine, quinine, and mefloquine, are all toxic to the blood stage parasite. The mechanism of action of these drugs is not well understood, although they have been hypothesized to interfere with hemoglobin digestion and heme detoxification within the parasite [5–7].

The heme detoxification pathway of *P. falciparum* is a particularly attractive drug target: (1) it targets the parasites at the stage when they are causing the clinical pathologies; (2) humans detoxify free heme via the heme oxygenase/biliverdin reductase pathway; hence, a drug that interferes with heme processing in *P. falciparum* will not inhibit heme detoxification in humans; and (3) inhibition of heme detoxification would lead to a build-up of high concentrations of toxic free heme inside the parasite.

One protein that has been implicated in heme detoxification within *P. falciparum* is histidine-rich protein 2 (HRP-2), a 30 kDa protein consisting of 35% histidine residues [8, 9]. HRP-2 has been shown to bind multiple molecules of heme and to mediate heme polymerization in vitro [10, 11]. We have previously demonstrated that HRP-2 can bind heme via bis-histidyl coordination [11]. Compounds that either inhibit heme binding to HRP-2 or inhibit polymerization of heme bound to HRP-2 should be toxic to the parasite. Inhibition of heme binding could occur in two ways. Inhibition could occur via the sequestration of heme in solution by the formation of semistable solution complexes. Complexes of this type have been reported with the antimalarial chloroquine [12–14], and we have evidence that chloroquine inhibits heme binding to HRP-2 by this mechanism (our unpublished results). Alternatively, inhibition could come about by compounds binding to the HRP-2 heme complex or to HRP-2 alone, thereby preventing heme from binding (Figure 6). Here, we present our data describing (1) identification of compounds that inhibit heme binding to HRP-2 and (2) the effects of these heme binding inhibitors on parasite growth.

In order to screen a large number of compounds, we

[5]Correspondence: marletta@cchem.berkeley.edu

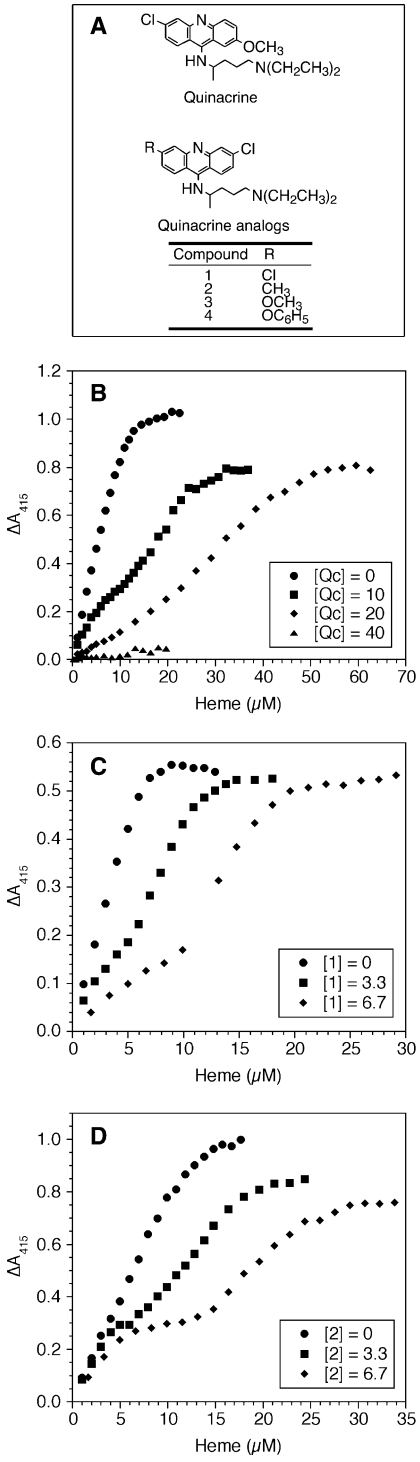

Figure 1. The Effect of Quinacrine and Analogs on Heme Binding

The chemical structures of quinacrine and the analogs used are shown in (A). Effects of (B) quinacrine (Qc), (C) Compound **1**, and (D) **2** on HRP-2-heme binding using the heme titration experiment as described under Experimental Procedures. Heme was simultaneously titrated into both the experimental cuvette (containing 0.2 μM HRP-2 and varying concentrations of the test compound) and a reference cuvette (containing the test compound), and difference absorption spectra were recorded. The *y* axis is the λ_{max} of the difference spectra (located at 415 nm). The concentrations of each compound in μM are given in the insets.

have developed a novel microplate-based assay that provides a method for a quick and efficient screen. Using this assay, we found several compounds that strongly inhibit heme binding to HRP-2. These compounds were also screened in bioassays to determine their ability to inhibit parasite growth. The results of these two methods revealed a strong correlation between inhibition of heme binding and inhibition of parasite growth.

Results

Heme Binding Assay

HRP-2-bound heme has a Soret peak at 414 nm, while free heme (i.e., unbound to HRP-2) has a broad, low-extinction Soret peak centered around 386 nm. In the heme binding assays described here, heme binding to HRP-2 was followed by monitoring the increase in the Soret absorbance caused by heme binding. Absorbance contributions from the test compounds and free heme have been subtracted. Inhibition of, or interference with, heme binding led to a decrease in the Soret at 414 nm.

Screening of Acridine Derivatives

We obtained several chloroquine and quinacrine analogs from the library of compounds at Parke-Davis Pharmaceutical Co. (now Pfizer Global Research & Development). Compounds **1**, **2**, **3**, and **4** appeared to be the most potent inhibitors of heme binding. These acridine derivatives are shown in Figure 1A. The potency of compounds **1–4** to inhibit heme binding to HRP-2 was compared with quinacrine, an acridine-based antimalarial drug. Results of the heme titration experiments using quinacrine, **1**, and **2** are shown in Figures 1B, 1C, and 1D, respectively. Heme titration results for **3** and **4** are very similar to Figures 1C and 1D (data not shown). Compounds **1–4** are about 3-fold more potent than quinacrine. As shown in Figure 1, the addition of more heme overcomes the inhibition. The heme titration results in Figure 1 are not simple linear decreases in absorbance, suggesting that the inhibition of heme binding is complicated and could likely involve, in part, a heme-compound complex in solution.

The effects of compounds **1** and **2** on parasite growth were examined. The two compounds were tested against both the chloroquine-sensitive (HB-3) and the chloroquine-resistant (Dd-2) strains. Compound **1** inhibited the growth of *P. falciparum* cultured in erythrocytes, with IC_{50} value of 40 nM against both the chloroquine-sensitive and the chloroquine-resistant strains. The IC_{50} values for compound **2** were determined to be 50–100 nM and 100 nM against the chloroquine-sensitive and -resistant strains, respectively.

Library Development and Screening

A combinatorial library based on general structure **5** (Figure 2) was produced with the initial goal of targeting plasmepsin II, a parasite aspartyl protease that cleaves hemoglobin in the *P. falciparum* food vacuole. A minor byproduct, **6**, was identified as a very weak inhibitor of the plasmepsin II (IC_{50} = 20 μM) yet was quite potent against the parasite in cell culture ($IC_{50} \approx$ 100 nM). As expected, removal of the stereospecific functional

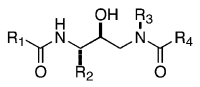

5

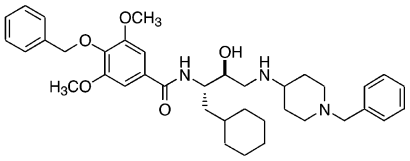

6

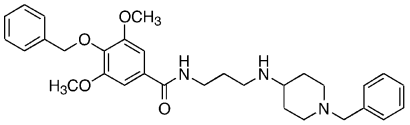

7

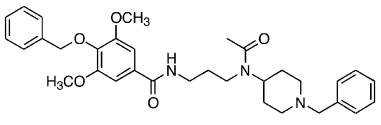

15

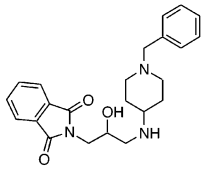

35

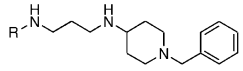

Compound	R
8	[1-naphthyl]OCH_2CO
9	3-pyridyl-CO
10	C_6H_5CO

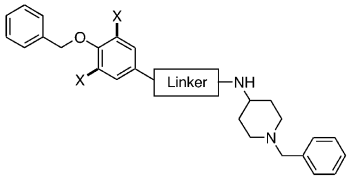

Compound	X	Linker
11	OCH_3	$CONH(CH_2)_4$
12	OCH_3	$CH_2O(CH_2)_3$
13	H	$NHCO(CH_2)_2$
14	H	$CH_2NHCO(CH_2)_2$
35	OCH_3	$CH_2NH(CH_2)_4$

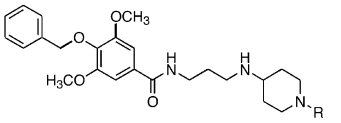

Compound	R
16	$(C_6H_5)_2CHCH_2$
17	$C_6H_{11}CH_2$
18	$C_6H_5C_6H_4CH_2$
19	3,4-(methylenedioxy)$C_6H_3CH_2$
20	CH_3
36	(1-Me-3-indol)CH_2

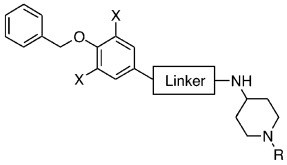

Compound	X	Linker	R
21	H	$NHCO(CH_2)_2$	$CH_2C_6H_{11}$
22	H	$NHCO(CH_2)_2$	$CH_2CH(C_6H_5)_2$
23	H	$CH_2NH(CH_2)_3$	$COCH_2C_6H_5$
24	H	$CH_2NH(CH_2)_3$	$CH_2CH(C_6H_5)_2$
32	OCH_3	$CONH(CH_2)_3$	H

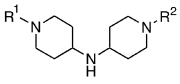

Compound	R^1	R^2
25	CH_2CH_2*p*-C_6H_4Cl	CH_2CH_2*p*-C_6H_4Cl
26	$CH_2CH(C_6H_5)_2$	$CH_2CH(C_6H_5)_2$
27	$CH_2CH(C_6H_5)_2$	$CH_2C_6H_4OCH_2C_6H_5$
28	CH_2CH_3	$CH_2CH(C_6H_5)_2$
29	$CH_2CH_2C_6H_5$	$CH_2CH_2C_6H_5$
30	$CH_2C_6H_5$	$CH_2C_6H_5$
31	$CH_2C_6H_{11}$	$CH_2C_6H_{11}$
34	$CH_2CH_2C_6H_{11}$	$CH_2CH_2C_6H_{11}$

Figure 2. General Structure of the Combinatorial Library and the Library-Derived Compounds

Structure **5** was the initial template for library design. Structure **6**, a by-product of the synthesis, was determined to be active in parasite killing but a weak plasmepsin inhibitor. Removal of the stereospecific centers yields structure **7**. The general synthetic routes for the combinatorial library-derived compounds are described in the Experimental Procedures section. The classes of compounds shown under each section were developed from the lead compound **7**.

groups from the compound (**7** in Figure 2) resulted in a molecule that was a very poor inhibitor of plasmepsin II (IC_{50} >250 μM). Interestingly, this and others in this class retained the ability to inhibit parasite growth, indicating that the targeted proteases were not responsible for the inhibition of parasite growth. Based on this observation, more compounds were generated using combinatorial chemistry methods.

Using the microplate heme binding assay, we screened the compounds shown in Figure 2 and compared these results with those obtained from the parasite growth-inhibition assays. Figures 3A and 3B are representative heme binding assay results. In each case, heme binding is plotted against the concentration of heme alone and in the presence of a test compound. In the absence of test compound, the heme binding curve shows an increase in ΔA_{Soret} as the concentration of heme increases, followed by a plateau as the heme binding sites become saturated. A concentration-dependent decrease in ΔA_{Soret} is indicative of concentration-dependent inhibition.

An example of a potent heme binding inhibitor (compound **24**) is shown in Figure 3A. The ΔA_{Soret} is minimal at the three concentrations tested and is essentially zero at 100 μM, indicating that heme binding to HRP-2 has been almost completely inhibited. Compound **10** is an example of a weak inhibitor. As seen in Figure 3B, compound **10** has little influence on the binding curve, indicating that **10** is unable to interfere with heme binding to HRP-2.

The potency of each compound to inhibit heme binding to HRP-2 was determined by calculating percent inhibition that resulted at a 1:1 ratio of compound to heme as follows:

$$\% \text{ inhibition} = (\Delta A_{\text{No Compound}} - \Delta A_{\text{With Compound}})/(\Delta A_{\text{No Compound}}) \times 100$$

All of the results of the microtiterplate heme binding assay and the IC_{50} values obtained from parasite growth inhibition studies are compiled in Table 1. A plot of percent inhibition versus IC_{50} was constructed (Figure 3C) in order to determine if there is a correlation between the ability of each compound to inhibit parasite growth in culture and the ability to inhibit heme binding to HRP-2.

For most of the compounds tested, their ability to inhibit heme binding is a good predictor of the antiparasitic potency. Those compounds that are strong inhibitors of heme binding, such as **16**, **22**, and **24–27**, are potent inhibitors of parasite growth, having IC_{50} values in low nanomolar range. Alternatively, **9**, **10**, **15**, **32**, and **33** are weak inhibitors of both heme binding and parasite growth. There were no examples of compounds that were more potent against the CQ-resistant strain that were also potent in the heme binding assay. In the CQ-resistant strain, compounds were either equally potent or less potent in parasite killing.

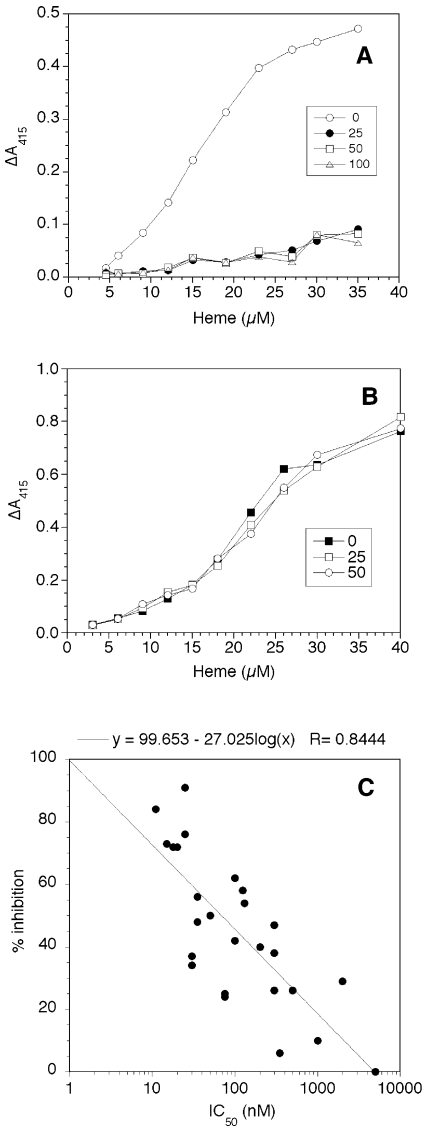

Figure 3. Heme Binding Inhibition Assay and the Relationship to Parasite Growth

Effects of (A) a strong inhibitor, compound **24**, and (B) a weak inhibitor, **10**, on heme binding by HRP-2 using the microtiterplate assay described under Experimental Procedures. Compound concentrations are given in the insets. The relationship of heme binding to parasite growth is shown in (C). The *y* axis refers to the results of the microplate heme binding assay expressed as percent inhibition at 1:1 ratio of the concentrations of the test compound to heme (typically between 30–40 μM). The *x* axis refers to the results of the parasite growth-inhibition assay. Points shown in closed circles were fitted to the equation $y = 99.653 - 27.025 \log(x)$, $r^2 = 0.844$.

Mechanism of Inhibition

Figure 6 depicts the several possible ways that compounds might interfere with heme binding to HRP-2. As mentioned, CQ is thought to act by forming a relatively stable solution complex with heme and in doing so exposes the parasite to the toxic properties of free heme in solution. Several of the compounds derived from the combinatorial library work by forming a solution complex with heme. Shown in Figure 4A are the results with compound **24**. The increase in absorbance at 429 nm is similar to the solution complex seen between CQ and heme. This suggests that some of the active compounds may work via a similar mechanism. Some of the less potent compounds do not induce the same spectral

Table 1. Results of Parasite Growth-Inhibition Assays and Microtiterplate Heme Binding Inhibition Assays

Compound	IC_{50} (nM)[a] CQ-Sensitive Strain	IC_{50} (nM)[a] CQ-Resistant Strain	Heme Binding[b] Inhibition %
8	350		6
9	>5000		0
10	>5000		0
11	300		47
12	500		26
13	75		25
14	200	–	40
15	>5000	–	0
16	15	200	73
17	30	350	37
18	50		50
19	75		24
20	2000		29
21	100	–	62
22	18	130	72
23	125	–	58
24	11	70	84
25	20	80	72
26	25	45	76
27	25	75	91
28	>100	>200	42
29	130	>200	54
30	>300	>300	26
31	>300	>300	38
32	>1000		10
33	>5000		0
34	35		56
35	35		56
36	35	150	48

[a] The concentration of the test compound that inhibited parasite growth by 50% by the method described in Experimental Procedures.

[b] The inhibition of heme binding as determined by the microtiterplate assay described in Experimental Procedures. The values listed are the percent inhibition observed at an equimolar ratio of compound to heme.

shift. We further explored potential mechanisms of inhibition outlined in Figure 6 by testing if heme could reverse the inhibitory effect. The results of the heme reversal experiment with **24** are shown in Figure 4B. It is clear from this experiment that heme reverses the inhibition. If the inhibitory effect was due to the formation of a stable solution complex between heme and **24** (complex [B] in Figure 6), then we would expect to see results like those in Figure 4A. However, we cannot rule out the participation of complexes [C] and [D], since we have no measure of the relative affinities in question. In fact, when an experiment like that in Figure 4A was carried out with a weak inhibitor, **10**, there was a much weaker intensity peak at ~429 but a significant decrease in the heme absorption in the sample, suggestive of a heme-compound complex but not as strong and certainly different than that which forms with strong inhibitors (data not shown). The complex that forms with weak inhibitors such as **10** also seems to form more slowly (data not shown). The overall conclusion is that there are likely to be multiple mechanisms of inhibition, and the current assays do not help to distinguish among the possibilities.

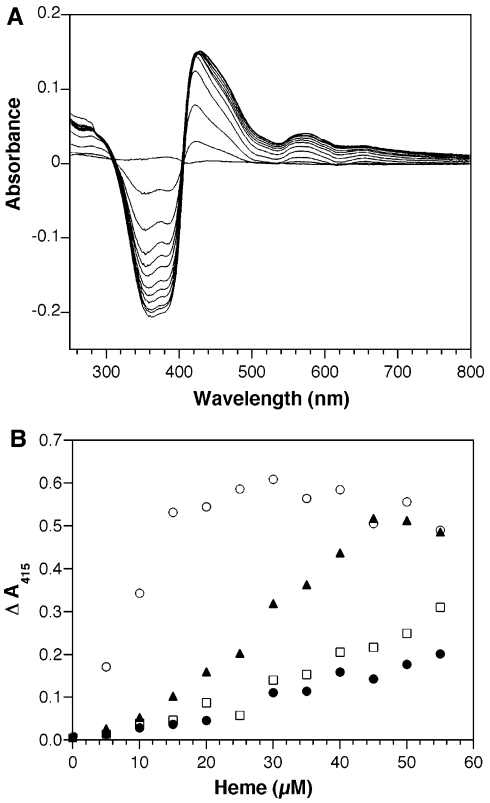

Figure 4. Probing the Mechanism of Action of Compound **24**

(A) Formation of a complex between **24** and heme. Compound **24** was titrated into a heme solution as described under Experimental Procedures. Addition of compound resulted in a peak at 421 nm, similar to that seen between chloroquine and heme. Higher concentrations of compound shift the peak maximum to 429 nm.

(B) Microtiterplate heme binding inhibition assay with compound **24**. Heme concentrations of up to 55 μM were used with no compound (open circles), 10 μM compound (filled triangles), 25 μM compound (open squares), and 50 μM compound (filled circles). With increased addition of heme, inhibition by the compound is overcome, and the ΔA_{415} increases to levels similar to those reached in the absence of compound.

Discussion

Microplate Heme Binding Inhibition Assay

With the rise of drug resistance to the commonly used antimalarial drugs, there is a critical need for novel antimalarial drug development and consequently a need for novel potential targets. The heme detoxification pathway of *P. falciparum* has been studied in this context. This pathway meets two important criteria for an ideal drug target: (1) it is unique to the parasite, and (2) it is required for parasitic survival. HRP-2 appears to be intimately involved in heme processing. First, HRP-2 has a large capacity for binding free heme [11]. The ability of HRP-2 to act as a heme sponge may be its most important function since the parasite is exposed to high heme concentrations via the catabolism of hemoglobin. Second, once it binds heme, HRP-2 appears to play a role in heme polymerization, thereby detoxifying free heme [10]. It follows, then, that compounds that interfere with HRP-2 heme binding would lead to an increase in

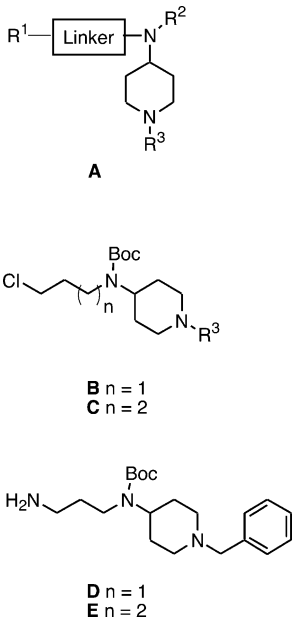

Figure 5. Synthetic Precursors

Compounds synthesized in the combinatorial synthesis were derived from these synthetic precursors.

free heme concentration and should therefore be toxic to the parasite.

In order to facilitate screening of compounds that can inhibit heme binding to HRP-2, we developed a quick, efficient, and inexpensive method of screening a large number of compounds. These compounds should also inhibit heme polymerization and therefore act as antimalarials. Bioassays, such as the parasite growth inhibition assay that monitors the effects of small molecules on the growth of cultured parasite, are labor intensive, expensive, and slow, prohibiting screening of a large number of compounds. Moreover, the results of growth inhibition studies do not provide any information about either the target or the mode of action of a drug. The microplate-based assay reported here allows for an easy, efficient, and quick method of screening a large number of compounds.

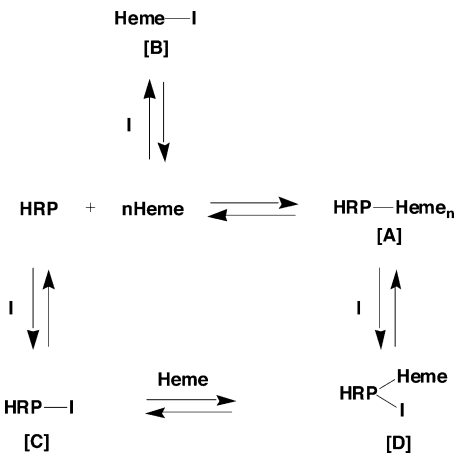

Figure 6. Inhibition of Heme Binding to HRP-2

This scheme depicts the potential mechanisms by which heme binding could be inhibited. Formation of complex [A] would lead to a loss in the ΔA_{415}. This could occur by formation of complex [B], and some of the compounds used in this study appear to act in this way. The inhibition results do not rule out inhibitory action by reversing complex [C] or [D].

There are many important advantages to monitoring heme binding rather than heme polymerization. First, heme binding is a very rapid process: at pH 7.0, heme binding by HRP-2 is complete within the mixing time. Heme polymerization, on the other hand, is a much slower process, requiring several hours. There are several conflicting reports about the reaction conditions and the time required for heme polymerization. Most report reaction time of 12–18 hr [10, 15, 16]. The fastest reaction time reported thus far is 30 min at 60°C [17]. However, reports from other groups [18] and our own work cannot duplicate heme polymerization under these conditions (data not shown). Second, in addition to being slow, using heme polymerization to screen potential antimalarial drugs is cumbersome, as several wash steps are required to separate free heme from polymerized heme once the polymerization reaction has been terminated [10, 15, 16]. The heme binding inhibition assay described here, on the other hand, requires no handling steps other than adding HRP-2, heme, and the test compound. No additional wash steps are necessary. Third, experiment-to-experiment variability is minimal using the microplate heme binding assay. Conversely, the number of wash steps required to separate free heme introduces additional sources of error to the heme polymerization assay; hence, experiment-to-experiment variability can be significant. We did find, however, that the most consistent results with the microplate assay were obtained when the protein was added last. As mentioned above (and shown in Figure 6), inhibition is not simple and some complexes that do form tend to precipitate. Spectral titrations generally reflect this complexity, and consequently comparisons of compound families are difficult. There are clear cases when part of the inhibition mechanism is due to a solution complex between the test compound and heme and other cases where the compound leads to either heme or protein precipitation (data not shown).

9-Aminoquinoline Compounds

Quinacrine is a 9-aminoacridine derivative that had been widely used to treat malaria until it was replaced by chloroquine in the 1940s. The mechanism of action of quinacrine is unknown [5]; however, the fact that quinacrine, 4-aminoquinolines (e.g., chloroquine), cinchona alkaloids (e.g., quinine), and quinolinemethanols (e.g., mefloquine) all share certain structural features (i.e., a hydrophobic, planar heterocyclic ring with a functional group containing a weakly basic nitrogen atom) suggests that they may share some similarities in their mechanism of action. Previous work has suggested that mechanism of action of chloroquine, mefloquine, and quinine may involve (1) interaction of these compounds with free heme [19, 20] and (2) subsequent inhibition of heme polymerization [5, 21, 22]. However, this hypothe-

sis remains unproven and the correlation between binding to heme and blockade of polymerization is inconsistent [12].

The data presented here clearly demonstrate that quinacrine can inhibit heme binding to HRP-2, although the plate assay does not clarify the mechanism of this inhibition. This finding supports the proposal that the in vivo mechanism of action of quinacrine involves interference with heme detoxification. The four 9-aminoacridines that we found to be even more potent (by about 3-fold) than quinacrine in their ability to inhibit heme binding suggests that modification of both the position and the nature of the substituents on the heterocyclic ring can lead to increased potency. Compounds **1–4** discussed here all have very similar heme binding curve profiles, indicating that a chloro-, methyl-, methoxy-, or phenoxy- group at the C–6 position makes little difference in their ability to inhibit heme binding.

Both compounds **1** and **2** were toxic to the chloroquine-sensitive and chloroquine-resistant strains, with **1** having an IC_{50} value that is 2-fold less than that of **2**. The observation that both compounds were similarly effective against the chloroquine-resistant strain as the chloroquine-sensitive strain could be important in the effort to treat chloroquine-resistant organisms.

Combinatorial Library Compounds

Though this new class of compounds is structurally unrelated to aminoquinolines, they possess a basic amine, a functionality thought to be important in chloroquine accumulation inside the food vacuole. Additionally, they all possess heterocyclic ring systems. As the food vacuole is the site of hemoglobin catabolism as well as heme detoxification, we tested the possibility that these compounds could be playing a role by interfering with heme processing. Using the heme binding inhibition assay described here, we screened all of the compounds for their ability to inhibit heme binding by HRP-2.

The results of the heme binding assay and the parasite growth-inhibition assay demonstrated that antiparasitic potency correlated well with the ability of these compounds to inhibit heme binding to HRP-2 (Figure 3C). The mode of action of many of the antiplasmodial agents effective against the blood-stage parasite are thought to involve hemoglobin degradation, heme, or heme detoxification. For instance, it has been hypothesized that quinoline-containing antimalarial drugs, such as chloroquine, quinine, and mefloquine, interfere with heme detoxification. Though none of the compounds in this new class structurally resemble quinoline-containing antimalarial drugs, there is a good correlation between the IC_{50} values and the level of heme binding inhibition. Though not definitive, this finding is certainly suggestive of the heme detoxification pathway being involved in the mode of action of these compounds. Likewise, it remains to be determined whether the heme binding inhibitors act by (1) interacting with HRP-2, thereby prohibiting HRP-2 from binding heme; or (2) interacting with heme, thereby sequestering heme from binding HRP-2 (Figure 6).

Several of these compounds (**24–27**) retain their potency against the chloroquine-resistant strain. All have IC_{50} values below 100 nM against the chloroquine-resistant strain and IC_{50} values under 30 nM against the chloroquine-sensitive strain.

It is interesting that these new compounds are more potent against the chloroquine-sensitive strain than the resistant strain, even though they are structurally unrelated to chloroquine. In particular, **16** and **17** have antiplasmodial potency that is at least 10-fold weaker in the chloroquine-resistant strain then it is in the chloroquine-sensitive strain. Possibly, there may be some crossresistance such that the mechanism that confers chloroquine resistance may affect these compounds as well.

As mentioned above, the resistance of *Plasmodium falciparum* to commonly used drugs such as chloroquine and related compounds will seriously hamper the ability to treat and control the disease that afflicts millions every year. Rational drug design has not played a very important role in treating malaria. The *Plasmodium* sequencing project underway will be an important step in providing novel targets for new pharmaceuticals. Heme polymerization is clearly important to the organism, and here we have demonstrated the utility of the microtiterplate heme binding inhibition assay as a first-line screening tool for target-based drug design, targeting the HRP-2-mediated heme detoxification pathway of *P. falciparum*. The microtiterplate heme binding assay makes screening of a large number of compounds possible. Moreover, the heme binding assay seems to correlate reasonably well with the inhibition of parasite growth. As we have reported here, potent new compounds to treat the disease have been found and represent a new direction in treating this disease.

Significance

Malaria continues to be one of the most common human infections, responsible for 1–2 million deaths per year. While effective treatments exist, resistance to commonly used drugs such as chloroquine clearly indicates that novel therapies must be developed. The histidine-rich proteins, typified by HRP-2, are a unique class of proteins that act as a heme sponge and mediate the formation of hemozoin, the catabolic, dimeric end product of heme metabolism in the parasite. Interference in this detoxification pathway is important to parasite survival, especially during the blood-stage infection, when catabolism of hemoglobin serves as the nutrient source. With the development of a microtiter plate assay for inhibition of heme binding to HRP-2, we have explored the relationship of the inhibition of heme binding to HRP-2 to parasite killing, primarily using a portion of a combinatorial library developed against the parasite. Our results show that parasite killing is directly correlated to interference with heme binding to HRP-2 and suggest further that inhibition of heme binding to HRP-2 may be the mechanism of action of chloroquine. Taken together, our results point the way toward novel therapies to treat this important human disease.

Experimental Procedures

Materials

HRP-2 was expressed and purified as described previously [10, 11]. Compounds **1–4** were a generous gift from Parke-Davis Pharmaceu-

tical (now Pfizer Global Research & Development). Ninety-six-well, flat-bottom microplates were from Costar. All other chemicals were purchased from Sigma Chemical Co. (St. Louis, MO) unless otherwise stated.

Materials for synthesis: ion exchange resin (AG MP-50, cat. no. 143-0841) was purchased from Bio-Rad. Anhydrous *N,N*-dimethyformamide (DMF) was purchased from Aldrich. Chloroform ($CHCl_3$) was passed through basic alumina prior to use. Flash column chromatography was carried out with Merck 60 230-400 mesh silica gel. ^1H- and ^{13}C-NMR spectra were recorded using a UCB Bruker AMX-400 and AM-400 spectrometers.

Chemistry

The new class of antimalarials was built around a common basic structure **A** (Figure 5) containing four sites of possible diversity (i.e., R^1, linker, R^2, and R^3). A brief summary of the synthetic scheme is included here. A more detailed description of the synthesis with complete compound characterization will be reported elsewhere [25].

R^1 Site Modification

Synthesis of Compounds 8–10

(1) 4-amino-1-benzylpiperidine was reacted with 1-bromo-3-chloropropane in CH_3CN. (2) The product from step 1 was then treated with di-*t*-butyl dicarbonate in THF and purified on a silica gel column to generate **B** (where $R^3 = CH_2C_6H_5$) (refer to Figure 5). (3) **B** ($R^3 = CH_2C_6H_5$) was treated with NaN_3 and NaI in DMF. (4) $SnCl_2$, PhSH, Et_3N, and the intermediate from step 3 were added together in THF to produce **D** (refer to Figure 5). (5) **D** was treated with a variety of carboxylic acids (i.e., R^1CO_2H) and applied to solid supported EDC (P-EDC). Removal of the Boc group and purification of the products were simultaneously achieved using a strongly acidic ion exchange resin (P-SO_3H). Next, NH_3/MeOH was applied to the amine-bound resin to release the free amine products **8–10**.

Linker Modification

Amide (11)

4-benzyloxy-3,5-dimethoxybenzoic acid was coupled to amine **E**, which was prepared according to the sequence described for **D**, except that 1-bromo-4-chlorobutane was used in place of 1-bromo-3-chloropropane. The acid and **E** were coupled, and then the product was deprotected to provide **11** exactly according to the protocols used to prepare products **8–10**.

Ether (12)

4-benzyloxy-3,5-dimethoxy-alcohol was treated with NaH followed by alkyl chloride **B** ($R^3 = CH_2C_6H_5$). The Boc group was removed as described previously to generate **12**.

Reverse Amide (13, 21, and 22)

4-benzyloxyaniline was coupled with N-Boc-β-alanine. After cleavage of the Boc group, *N*-R^3-piperidone was added and the mixture was treated with $NaHB(OAc)_3$ to generate compounds **13**, **21**, and **22**. (R^3 is $CH_2C_6H_5$ for compound **13**, $CH_2C_6H_{11}$ for compound **21**, and $CH_2CH(C_6H_5)_2$ for compound **22**.)

Reverse Amide (14)

4-benzyloxybenzylamine was coupled with N-Boc-β-alanine. After cleavage of the Boc group, *N*-benzyl-piperidone was added and the mixture was treated with $NaHB(OAc)_3$ to generate compound **14**.

R^2 Site Modification

Synthesis of Compound 15

4-benzyloxy-3,5-dimethoxybenzoic acid was coupled to **7**. After Boc deprotection, the R^2 site modification was achieved by treating this intermediate with acetyl chloride to generate compound **15**.

R^3 Site Modification

Synthesis of Compounds 16–20, 32, 36

(1) Compound **B** ($R^3 = CH_2C_6H_5$) was *N*-debenzylated using H_2, Pd/C, AcOH, and EtOAc. (2) To the intermediate produced in step 1 was added Et_3N and allyl chloroformate. (3) The product purified from step 2 was treated with NaN_3 and NaI in DMF to generate the azide adduct. (4) Treatment of the azide-containing intermediate from step 3 with $SnCl_2$, PhSH, and Et_3N provided the free amine, which was coupled with 4-benzyloxy-3,5-dimethoxybenzoic acid. (5) The Alloc protection group from the step 4 intermediate was removed using standard Pd(0) catalyzed methods, and the resulting amine was treated with various aldehydes under reductive conditions ($NaBH_3CN$). Simultaneous removal of the Boc group and purification of the products was achieved using a strongly acidic ion exchange resin (P-SO_3H). Finally, NH_3/MeOH was applied to the amine-bound resin to release the free amine (compounds **16–20**, **36**). Removal of the Boc group from the intermediate from step 4 directly generates **32**.

Synthesis of Compound 23

(1) Compound **B** ($R^3 = CH_2C_6H_5$) was *N*-debenzylated (using H_2, Pd/C, AcOH, and EtOAc) and coupled to $C_6H_5CH_2CO_2H$, thereby generating an *N*-acylated piperidine. (2) Next, the product of step 1 was treated with NaN_3 and NaI in DMF to generate the azide adduct. (3) Reduction of the azide-containing intermediate from step 2 was followed by reductive amination with 4-benzyloxy-1-benzaldehyde. (4) The Boc group was removed to yield compound **23**.

Synthesis of Compound 24

(1) Compound **B** ($R^3 = CH_2C_6H_5$) was *N*-debenzylated using H_2, Pd/C, AcOH, and EtOAc. (2) To the intermediate produced in step 1 was added Et_3N and allyl chloroformate. (3) The product purified from step 2 was treated with NaN_3 and NaI in DMF to generate the azide adduct. (4) Treatment of the azide-containing intermediate from step 3 with $SnCl_2$, PhSH, and Et_3N provided the free amine, which was coupled with 4-benzyloxy-benzoic acid. (5) The Alloc protection group from the step 4 intermediate was removed using standard Pd(0) catalyzed methods, and the resulting amine was treated with $(C_6H_5)_2CHCH_2CHO$ under reductive conditions ($NaBH_3CN$). Simultaneous removal of the Boc group and purification of the products was achieved using a strongly acidic ion exchange resin (P-SO_3H). The amide was then reduced to the corresponding amine using $LiAlH_4$ in THF.

Synthesis of Compound 33

Compound **33** was obtained in two straightforward steps by Mitsunobu reaction (DIAD, Ph_3P, THF) of (*R*) glycidol with phthalimide followed by epoxide opening with 1-*N*-benzyl-4-aminopiperidine.

Synthesis of Compounds 25–31, 34

(1) Treatment of 4-amino-1-benzylpiperidine with di-*t*-butyl dicarbonate in THF provides the *N*-Boc protected material. (2) Treatment of the intermediate from step 1 with Pd/C and H_2 provides the secondary amine, which is coupled with a variety of aldehydes [$ClC_6H_4CH_2CHO$, $(C_6H_5)_2CHCHO$, C_6H_5CHO, $C_6H_{11}CHO$, and $C_6H_{11}CH_2CHO$] under reductive conditions ($NaBH_3CN$). The intermediate from step 2 is then treated under reductive conditions ($NaBH_3CN$) with *N*-substituted 4-piperidones [*N*-substitution is CH_3CH_2-, $ClC_6H_4CH_2CH_2$-, $(C_6H_5)_2CHCH_2$-, $C_6H_5CH_2$-, $C_6H_{11}CH_2$-, and $C_6H_{11}CH_2CH_2$-] to provide **25–31**, **34**.

Amine (35)

11 was reduced using $LiAlH_4$ in THF.

Heme Titration

All electronic absorption spectra were recorded on a Cary 3E (double beam) spectrophotometer with the temperature set at 37°C using a Neslab RTE-100 temperature controller.

A stock solution of 1 mM heme was made in 0.1 M NaOH, and its concentration was determined spectroscopically ($\epsilon_{385} = 58.44\ mM^{-1}cm^{-1}$) [23]. This heme solution was simultaneously titrated into two cuvettes. One cuvette contained 0.2 μM HRP-2 and varying concentrations of the test compound in 100 mM HEPES (pH 7.0). The second cuvette, the reference cuvette, contained only the test compound in equal concentration as the first cuvette. Heme was added in 1 μM increments, and difference absorption spectra were recorded after each addition. The difference spectra had a peak at 416 nm and a trough at 368 nm. The heme binding curve was constructed by plotting ΔA_{415} versus the heme concentration.

Compound Titration

All electronic absorption spectra were recorded on a Cary 300 spectrophotometer at 37°C. The sample and reference cuvettes contained 10 μM heme in 100 mM HEPES (pH 7.0). A stock solution of 2 mM test compound was prepared in 100 mM HEPES. The test compound was added in 2 μM increments to the sample cuvette. Difference absorption spectra were recorded after each addition.

Microtiterplate Inhibition Assay

Two 96-well, flat-bottom microplates were used per test compound. In one microplate, HRP-2, test compound, and heme were mixed in 250 μl total volume. The second microplate, the reference plate, contained only the test compound and heme (with identical concentrations as the first microplate). Each of the components were prepared as follows.

A stock solution of 1 mM heme was made in 0.1 M NaOH. This stock heme solution was serially diluted in 100 mM HEPES (pH 7.0) to the desired concentration. In a typical microtiterplate experiment, ten heme solutions, concentrations ranging from 0 to 100 μM, were used. In each well, 100 μl of each heme solution was added such that the final heme concentrations ranged from 0 to 40 μM.

A stock solution of each test compound was prepared in H_2O to 10 mM. These stock solutions were serially diluted in H_2O to the desired concentration (specific concentrations are described in the figure legends). Either the test compound or H_2O (50 μL) was added to each well.

HRP-2 was diluted to 2.5 times the desired final concentration using 100 mM HEPES (pH 7.0). HRP-2 concentration is specified in the figure legends, but 0.3 or 0.4 μM final concentration of HRP-2 was used for a typical experiment. Either HRP-2 or buffer (100 μL) was added to each well.

The assay components in each well were mixed thoroughly using the microplate reader. After incubating each microplate at room temperature for 10 min, the absorbance at 415 nm was measured. All samples were done in duplicate, and their values were averaged.

Heme binding to HRP-2 is monitored by observing the Soret peak absorbance [i.e., $A_{415\ (HRP\text{-}2\text{-}heme\text{-}test\ compound)}$]. Absorbance contributions from free heme and the test compound [i.e., $A_{415\ (heme\text{-}test\ compound)}$] are subtracted. A heme binding curve with no test compound added was run with each test compound. ΔA_{415} was plotted against the heme concentration to generate the heme binding curve at various test compound concentrations where:

$$\Delta A_{415} = A_{415}\ [\text{HRP-2-heme-test compound}] - A_{415}\ [\text{heme-test compound}]$$

Growth Inhibition Studies

All parasite growth inhibition studies were performed using the method described previously [24]. Effects of the various compounds on parasite growth were measured by monitoring the levels of ^{3}H-hypoxanthine incorporation by the late ring-stage parasite cultured in human erythrocytes.

Received: December 12, 2001
Revised: May 21, 2002
Accepted: June 5, 2002

References

1. Breman, J.G., Egan, A., and Keusch, G.T. (2001). The intolerable burden of malaria: A new look at the numbers. Am. J. Trop. Med. Hyg. *64*, iv–vii.
2. Krogstad, D.J. (1993). Blood and tissue protozoa. In Mechanisms of Microbial Disease, M. Schaechter, G. Medoff, and B.I. Eisenstein, eds. (Baltimore, MD: Williams and Wilkins), pp. 597–615.
3. Pagola, S., Stephens, P.W., Bohle, D.S., Kosar, A.D., and Madsen, S.K. (2000). The structure of malaria pigment beta-haematin. Nature *404*, 307–310.
4. Rosenthal, P.J., and Meshnick, S.R. (1996). Hemoglobin catabolism and iron utilization by malaria parasites. Mol. Biochem. Parasitol. *83*, 131–139.
5. Slater, A.F.G. (1993). Chloroquine: Mechanism of drug action and resistance in *plasmodium falciparum*. Pharmacol. Ther. *57*, 203–235.
6. Foley, M., and Tilley, L. (1998). Quinoline antimalarials: mechanisms of action and resistance and prospects for new agents. Pharmacol. Ther. *79*, 55–87.
7. Sullivan, D.J., Matile, H., Ridley, R.G., and Goldberg, D.E. (1998). A common mechanism for blockade of heme polymerization by antimalarial quinolines. J. Biol. Chem. *273*, 31103–31107.
8. Wellems, T.E., and Howard, R.J. (1986). Homologous genes encode two distinct histidine-rich proteins in a cloned isolate of *plasmodium falciparum*. Proc. Natl. Acad. Sci. USA *83*, 6065–6069.
9. Panton, L.J., McPhie, P., Maloy, W.L., Wellems, T.E., Taylor, D.W., and Howard, R.J. (1989). Purification and partial characterization of an unusual protein of *plasmodium falciparum*: Histidine-rich protein II. Mol. Biochem. Parasitol. *35*, 149–160.
10. Sullivan, D.J., Gluzman, I.Y., and Goldberg, D.E. (1996). Plasmodium hemozoin formation mediated by histidine-rich protein. Science *271*, 219–221.
11. Choi, C.Y.H., Cerda, J.F., Chu, H.-A., Babcock, G.T., and Marletta, M.A. (1999). Spectroscopic characterization of the heme-binding sites in plasmodium falciparum histidine-rich protein 2. Biochemistry *38*, 16916–16924.
12. Chou, A.C., Chevli, R., and Fitch, C.D. (1980). Ferriprotoporphyrin IX fulfills the criteria for identification as the chloroquine receptor of malaria parasites. Biochemistry *19*, 1543–1549.
13. Moreau, S., Perly, B., and Biguet, J. (1982). Interaction of chloroquine with ferriprotophorphyrin IX. Nuclear magnetic resonance study. Biochimie *64*, 1015–1025.
14. Vippagunta, S.R., Dorn, A., Matile, H., Bhattacharjee, A.K., Karle, J.M., Ellis, W.Y., Ridley, R.G., and Vennerstrom, J.L. (1999). Structural specificity of chloroquine-hematin binding related to inhibition of hematin polymerization and parasite growth. J. Med. Chem. *42*, 4630–4639.
15. Slater, A.F.G., Swiggard, W.J., Orton, B.R., Flitter, W.D., Goldberg, D.E., Cerami, A., and Henderson, C.B. (1991). An iron-carboxylate bond links the heme units of malaria pigment. Proc. Natl. Acad. Sci. USA *88*, 325–329.
16. Bohle, D.S., and Helms, J.B. (1993). Synthesis of β-hematin by dehydrohalogenation of hemin. Biochem. Biophys. Res. Commun. *193*, 504–508.
17. Egan, T.J., Hempelmann, E., and Mavuso, W.W. (1999). Characterization of synthetic β-haematin and effects of the antimalarial drugs quinidine, halofantrine, desbutylhalofantrine and mefloquine on its formation. J. Inorg. Biochem. *73*, 101–107.
18. Pandey, A.V., and Tekwani, B.L. (1996). Formation of haemozoin/β-haematin under physiological conditions is not spontaneous. FEBS Lett. *393*, 189–192.
19. Cohen, S.N., Phifer, K.O., and Yielding, K.L. (1964). Complex formation between chloroquine and ferrihaemic acid in vitro, and its effect on the antimalarial action of chloroquine. Nature *202*, 805–806.
20. Moreau, S., Perly, B., Chachaty, C., and Deleuze, C. (1985). A nuclear magnetic resonance study of the interactions of antimalarial drugs with porphyrins. Biochim. Biophys. Acta *840*, 107–116.
21. Slater, A.F.G., and Cerami, A. (1992). Inhibition by chloroquine of a novel haem polymerase enzyme activity in malaria trophozoites. Nature *355*, 167–169.
22. Chou, A.C., and Fitch, C.D. (1993). Control of heme polymerase by chloroquine and other quinoline derivatives. Biochem. Biophys. Res. Commun. *195*, 422–427.
23. Dawson, R.M.C., Elliot, D.C., Elliot, W.H., and Jones, K.M. (1995). Data for Biochemical Research (New York: Oxford University Press Inc.).
24. Gluzman, I.Y., Francis, S.E., Oksman, A., Smith, C.E., Duffin, K.L., and Goldberg, D.E. (1994). Order and specificity of the *plasmodium falciparum* hemoglobin degradation pathway. J. Clin. Invest. *93*, 1602–1608.
25. Kim, J.M. and Ellman, J.A. (2002). Novel and potent antimalarial agents. Bioorg. Med. Chem., in press.